



Published in final edited form as:

*Biomaterials*. 2015 July ; 58: 103–111. doi:10.1016/j.biomaterials.2015.04.033.

## Influence of molecular weight upon mannosylated bio-synthetic hybrids for targeted antigen presenting cell gene delivery

Charles H. Jones<sup>‡</sup>, Akhila Gollakota<sup>‡</sup>, Mingfu Chen, Tai-Chun Chung, Anitha Ravikrishnan, Guojian Zhang, and Blaine A. Pfeifer<sup>\*</sup>

Department of Chemical and Biological Engineering, University at Buffalo, The State University of New York, Buffalo, New York, USA

### Abstract

Given the rise of antibiotic resistant microbes, genetic vaccination is a promising prophylactic strategy that enables rapid design and manufacture. Facilitating this process is the choice of vector, which is often situationally-specific and limited in engineering capacity. Furthermore, these shortcomings are usually tied to an incomplete understanding of the structure-function relationships driving vector-mediated gene delivery. Building upon our initial report of a hybrid bacterial-biomaterial gene delivery vector, a comprehensive structure-function assessment was completed using a class of mannosylated poly(beta-amino esters). Through a top-down screening methodology, an ideal polymer was selected on the basis of gene delivery efficacy and then used for the synthesis of a stratified molecular weight polymer library. By eliminating contributions of polymer chemical background, we were able to complete an in-depth assessment of gene delivery as a function of (1) polymer molecular weight, (2) relative mannose content, (3) polymer-membrane biophysical properties, (4) APC uptake specificity, and (5) serum inhibition. In summary, the flexibility and potential of the hybrid design featured in this work highlights the ability to systematically probe vector-associated properties for the development of translational gene delivery candidates.

### Keywords

Gene therapy; nonviral vector; cationic polymers; antigen presenting cells; bactofection

---

<sup>\*</sup>Corresponding author. Department of Chemical and Biological Engineering, University at Buffalo, State University of New York, Buffalo, NY 14260-4200, USA, Phone: 716-645-1198, Fax: 716-645-3822. blainepf@buffalo.edu.

<sup>‡</sup>Equal contributions

**Publisher's Disclaimer:** This is a PDF file of an unedited manuscript that has been accepted for publication. As a service to our customers we are providing this early version of the manuscript. The manuscript will undergo copyediting, typesetting, and review of the resulting proof before it is published in its final citable form. Please note that during the production process errors may be discovered which could affect the content, and all legal disclaimers that apply to the journal pertain.

### ASSOCIATED CONTENT

Supplementary Information. Polymer synthetic scheme and additional hybrid characterization are available in the supplementary information.

### Author Contributions

The manuscript was written through contributions of all authors. All authors have given approval to the final version of the manuscript. The authors declare no competing financial interest.

## INTRODUCTION

The emergence of multidrug resistant pathogens highlights the inadequacies of current therapeutic options, thus prompting a shift from the use of active treatment regimens towards prophylactic alternatives. Of these, genetic vaccines are ideal candidates, as this vaccine variation offers the most flexibility in terms of antigen design, production, and storage potential [1]. Furthermore, genetic vaccines are predicated on the controlled introduction of genetic material into immune effector cells for the eventual induction of an adaptive immune response [2]. Driving this process is the choice of delivery vector that, unfortunately, is often associated with situationally-specific properties that do not permit ubiquitous usage. Accordingly, to address these and other concerns, we previously developed a hybrid bio-synthetic gene delivery vector that combined the vector-specific advantages and toolsets of bacteria and cationic polymers [3]. These normally separate vectors were also selected, in part, due to their independent records for stimulating adaptive immune responses [4–6].

The hybrid vector utilized the combination of an engineered *Escherichia coli* (*E. coli*) strain and a class of biodegradable cationic polymers, poly(beta-amino esters) (PBAEs). The polymer component was then further modified by the terminal conjugation of mannose to improve antigen presenting cell (APC) uptake specificity through CD206 stimulation. Although preliminary results indicated improved APC uptake and gene delivery, the analysis of a single polymer did not permit a comprehensive investigation of structure-function relationships or the effect of mannose inclusion. Thus, in the current study a library of structurally unique mannosylated PBAEs (PBAE-Mans) were prepared and analyzed for their potential use as a hybrid constituent. Upon identification of an optimal polymer, this specific polymer chemical background was further modified to elucidate the dependency of hybrid gene delivery improvements upon molecular weight and relative mannose content (independent of chemical composition). The results provide the first assessment of structure-function relationships for the development of next-generation hybrid bio-synthetic gene delivery vectors.

## MATERIALS AND METHODS

### Materials

Monomers were purchased from Sigma-Aldrich (St. Louis, MO). Acetone (HPLC), DMF (HPLC), and DMSO (99.7%), and cell culture components were purchased from Fisher Scientific (Pittsburgh, PA). Allyl alcohol (99%), D-(+)-mannose (cell culture grade) and 4-toluenesulfonyl chloride (p-TsCl) were purchased from Sigma-Aldrich. Phosphate buffered saline (PBS) and 3 M sodium acetate were purchased from Life Technologies (Grand Island, NY).

### Cell lines, Strains, and Plasmids

A murine RAW264.7 macrophage cell line kindly provided by Dr. Terry Connell (Department of Microbiology and Immunology, University at Buffalo, SUNY) was used for gene delivery assays. The cell line was maintained in medium prepared as follows: 50 mL of fetal bovine serum (heat inactivated), 5 mL of 100 mM MEM sodium pyruvate, 5 mL of 1 M

HEPES buffer, 5 mL of penicillin/streptomycin solution, and 1.25 g of D-(+)-glucose were added to 500 mL phenol red-containing RPMI-1640 and filter sterilized. Cells were housed in T75 flasks and cultured at 37°C/5% CO<sub>2</sub>.

YWT7-*hly* (BL21[DE3] background strain containing a chromosomally located copy of listeriolysin O [*hly*]) was selected as the bacterial vector for all gene delivery experiments [3, 7–9]. A luciferase reporter plasmid driven by a cytomegalovirus promoter (pCMV-Luc; Elim Biopharmaceuticals) was utilized during positive control transfection experiments and introduced to YWT7-*hly* via electroporation prior to bacterial or hybrid vector transfections. To assess bacterial membrane shearing (to be described below), a plasmid expressing blue fluorescent protein (BFP) (pB18cmBFPAzurite [10]) was transformed into YWT7-*hly* using electro-transformation.

### Mannosylated Poly(beta-amino esters) Synthesis

Polymers were synthesized using a previously developed three-step reaction [3, 4]. Briefly, diacrylate-capped polymers were first synthesized in DMSO at various diacrylate/amine molar ratios (D:A ratio) for 5 days at 60°C. The initial polymer library was synthesized using a 1.2 D:A ratio (Table 1); whereas, the expanded polymer set utilized a wider range (Table 2). Variance of molar ratios in the expanded polymer set permitted tunable control of the base polymer molecular weight (Table 2). All acrylate-terminated polymers were then reacted with excess ethylenediamine to amine-cap the terminal ends. Specifically, acrylate-terminated polymers were dissolved in DMSO at 167 mg/mL and reacted with 5 M ethylenediamine (in DMSO) at room temperature for 24 h. Amine-capped polymers were purified by dialysis followed by evaporation under vacuum. Dialysis procedures were conducted against acetone using molecular porous membrane tubing (Spectra/Por Dialysis Membrane, Spectrum Laboratories Inc.) with an approximate molecular weight cut off at 3,500 Da. As a last step, amine-capped PBAEs were then reacted with allyl- $\alpha$ -D-mannopyranoside (ADM) at a 1:2 molar ratio in DMSO at 90°C for 24 h and then purified via dialysis. Structure and purity of polymers were confirmed using <sup>1</sup>H NMR spectroscopy (data submitted or reported elsewhere [4]).

ADM was synthesized by dissolving 3 g of D-(+)-mannose and 18 mg p-TsCl in allyl alcohol (20 mL) at 90°C under reflux for 24 h. The reaction solution was then concentrated by vacuum distillation at 35°C.

### Preparation of Hybrid Vectors

Bacterial and hybrid vectors were prepared from bacterial cultures inoculated at 2% (v/v) from overnight starter cultures. Plasmid selection antibiotics were used as needed during bacterial culture within lysogeny broth (LB) medium. Following incubation at 36°C and 250 rpm until 0.4 to 0.5 OD<sub>600</sub>, samples were induced with 0.1 mM isopropyl  $\beta$ -D-1-thiogalactopyranoside (IPTG) at 30°C for 1 hr. Bacterial vectors were then washed once and standardized to 0.5 OD<sub>600</sub> in PBS; whereas, bacterial strains to be used in hybrid vector formation were washed once and standardized to 1.0 OD<sub>600</sub> in 25 mM NaOAc (pH 5.15). Polymer doses dissolved in chloroform were desiccated and resuspended in 25 mM NaOAc

(pH 5.15) prior to equal volume addition to 1.0 OD<sub>600</sub> bacterial strains. Hybrid vectors (final 0.5 OD<sub>600</sub>) and bacterial vectors in PBS were allowed to incubate at 22°C for 15 minutes.

### Hybrid Vector Characterization

Zeta potential of bacterial, polymer, and hybrid vectors was measured by dynamic light scattering (DLS). To measure surface hydrophobicity of bacteria before and after polymer additions, samples were analyzed using a modified microbial adhesion to hydrocarbon (MATH) assay [11, 12]. Briefly, bacterial and hybrid vectors were prepared and resuspended in PBS to a final 1.0 OD<sub>600</sub>. One milliliter of bacterial or hybrid vector solution was then added to a clean glass tube in addition to 110 µL of n-hexadecane (10% v/v). Each sample was vortexed for one minute at setting 10 (Analog Vortex Mixer, Fisher Scientific) and allowed 15 min for phase separation. Using a clean Pasteur pipet, bacterial/hybrid vector solution was retrieved, taking care to avoid the hydrocarbon layer, and transferred to a cuvette for a final OD<sub>600</sub> measurement. The percentage change of hydrophobicity is calculated by:

$$\Delta\text{Hydro}\% = \frac{(A_{\text{initial}} - A_{\text{final}})}{A_{\text{initial}}}$$

To quantify the degree of protein release from the bacterial vectors upon polymer surface additions, a BFP release technique was developed. Specifically, hybrid vectors were prepared as before using a bacterial strain carrying pB18cmBFP<sub>Azurite</sub> [10]. After a 30 min incubation, hybrid vectors were pelleted and the supernatant removed to analyze BFP release via 383/450 nm excitation/emission. The data presented was generated by taking raw measurements and background subtracting BFP-expressing, unperturbed bacterial vector readings.

### Transfection Studies

For gene delivery experiments, RAW264.7 cells were seeded into two different types of 96-well plates at  $3 \times 10^4$  cells/well in 100 µL antibiotic-free medium and incubated for 24 h to allow attachment. A tissue culture-treated, flat-bottom, sterile, white, polystyrene 96-well plate was used for luciferase assays; whereas, a tissue culture-treated, sterile, clear, polystyrene 96-well plate was used for bicinchoninic acid (BCA) assessment and a 3-(4, 5-dimethylthiazol-2-yl)-diphenyltetrazolium bromide (MTT) assay.

Hybrid vectors were diluted in antibiotic-free growth medium to a 10:1 multiplicity of infection (MOI; ratio of vectors to seeded macrophages). Following cellular attachment, macrophage medium was replaced with 50 µL of growth medium containing each respective vector and allowed to incubate for an hour. After incubation, 50 µL of gentamicin-containing growth medium was added to each well to eliminate external/non-phagocytized vectors. Following an additional 24 h incubation (48 h after initial seeding), plates were analyzed for luciferase expression using the Bright Glo assay (Promega) and protein content using the Micro BCA Protein Assay Kit (Pierce) according to each manufacturer's instructions. Similarly, FuGENE HD (Promega, Madison, WI) and JET-PEI were included as positive

transfection controls according to each manufacturer's instructions. Gene delivery was calculated by normalizing luciferase expression by protein content for each well/plate.

### Gene Delivery Inhibition Studies

To determine if transfection was affected by the presence of free mannose and physiological levels of serum, hybrid vectors were prepared as described above. Vectors were then transfected as before using RAW264.7 cells with the following alterations. First, 30 minutes prior to transfection, media was replaced with 50  $\mu$ L growth medium containing 1,000  $\mu$ M of free mannose and/or 50% v/v FBS. Transfection occurred as before except initial media was not replaced, but rather, hybrid vectors were added to yield a 100  $\mu$ L volume (and 150  $\mu$ L after incubation and gentamicin-containing medium addition).

### MTT Assay

Cytotoxicity resulting from hybrid vectors was determined by the MTT colorimetric assay. RAW264.7 cells were seeded and transfected as described above. Following a 24 h incubation after vector addition, cells were assayed with MTT solution (5 mg/mL), added at 10% v/v, for 3 h at 37°C/5% CO<sub>2</sub>. Medium plus MTT solution was then aspirated and replaced by DMSO to dissolve the formazan reaction products. Following agitated incubation for 1 h, the formazan solution was analyzed using a microplate reader at 570 nm with 630 nm serving as the reference wavelength.

### Statistical Evaluation

Unless otherwise indicated, data presented were generated from three independent experiments. Error bars represent standard deviation values. All statistical significance comparisons between groups were performed using a one-way ANOVA with Dunnett (to compare within groups) or Bonferroni (to compare across groups) post-tests.

## RESULTS AND DISCUSSION

### Polymer Synthesis and Characterization

The synthesis of the PBAE-Man polymers proceeds via a three-part conjugate (Michael) addition of amines to acrylate groups [4]. Utilizing our high-throughput polymer synthesis methodology, we produced 18 PBAE-Man polymers from a diverse set of monomers (Figure S1) [13–16]. The library was synthesized on a 1- to 2-g scale with increased monomer concentrations to provide greater control of stoichiometry, increase polymer molecular weight and end-group termination, and reduce potential intramolecular cyclization [15]. Upon identification of D4A4-Man as the optimal polymer (to be described below), the amine to diacrylate monomer (D4:A4) ratio was systematically varied (Figure S1, Step 1) to produce a second library of stratified molecular weight polymers with the same chemical background.

Each respective polymer structure and purity (from both polymer libraries) was confirmed using <sup>1</sup>H NMR (Previously reported [4] and data submitted). GPC and DLS were used to measure molecular weight, polydispersity index (PDI), and zeta potential (in two buffers) of the polymers (Tables 1 and 2). The generated polymer libraries spanned various chemical

backgrounds and molecular weights ranging from 6.8 to 33.7 kDa (weighted MW) while demonstrating broad PDI values (~1.2–2.5) characteristic of PBAEs. Following structure confirmation, each polymer library was evaluated for charge densities (zeta potential) in two physiologically-mimicking buffers. Both polymer libraries possessed negative charges in neutral buffer and cationic charges in acidic conditions. Furthermore, the zeta potential values of the D4A4 polymer library increased proportionally with increases in molecular weight regardless of buffer (Table 2).

### Bacterial Strain Generation

A single *E. coli* strain was selected as the bacterial vector based upon previous optimization studies [3, 7–9]. This particular bacterial strain was engineered to deliver a mammalian expression reporter plasmid (pCMV-Luc) with assistance of a chromosomal-located listeriolysin O (LLO) expression cassette driven by an inducible T7 promoter [17] at the *clpP* location [8].

### Hybrid Vector Formation and Characterization

Hybrid bio-synthetic vectors are formed through electrostatically-driven interactions between positively charged polymers (derived from protonated amines) and the negatively charged outer membrane of *E. coli* – enabling a simple mixing methodology and the potential for rapid vector formulation scalability. Moreover, previously we observed that surface deposition of cationic polymers to the bacterial core resulted in a beneficial attenuation phenomenon that was driven by a proposed membrane “integrative” model (data submitted). Specifically, polymer molecules are believed to first adsorb to the surface of bacteria prior to mediating mild disruptions of the outer and inner Gram-negative leaflet membranes through diffusive mechanisms. Thus, bacterial membrane destabilizations has been associated with improved gene delivery outcomes by facilitating the controlled release of internal protein and DNA cargo [7, 18].

Accordingly, the degree of polymer-mediated surface coverage was evaluated for bacterial membrane hydrophobicity increases and destabilization (Figure 1). Surface hydrophobicity was positively correlated with polymer dose and mannosylation (Figure 1, left panels). Mannosylation as a whole facilitated increased surface coverage. This may be the result of a shielding effect provided by mannose molecules that reduces charge-charge repulsion of discrete polymer molecules as they attach to the bacterial surface.

Following the “integrative” model, after surface deposition polymers were evaluated for their respective membrane destabilization potential via a novel colorimetric assay (as compared to our previous adsorption-based assessment of released protein and DNA [7]). Specifically, over-expression of BFP in *E. coli* prior to polymer addition provides a colorimetric molecule that will diffuse through polymer-mediated membrane disruptions. Membrane destabilization increases with mannosylation (Figure 1, right panels) independent of chemical background. In addition, for both polymer libraries, the polymer possessing the highest zeta potential (D3A5-Man) mediated the highest membrane destabilization. However, none of the polymers were able to facilitate complete disruption as demonstrated by a known membrane-active antibiotic (polymyxin B).

In addition to the bacterial effects upon polymer addition, the vector as a whole was evaluated for the macroscopic properties that are displayed to the environment. Namely, the zeta potential of hybrid vectors was evaluated at various polymers doses in two physiologically relevant pHs (Figure 2). Each pH represents either the extracellular environment (Figure 2B; neutral pH) or the phagolysosome (Figure 2A; acidic pH). Bacterial surface zeta potential increased positively with increasing polymer dose regardless of buffer or mannosylation. Hybrid vectors possessed the highest zeta potential values in the acidic condition, which presumably occurs due to protonation of amines on the polymer backbone. Generally, the mannosylated polymers possessed innate zeta potentials lower than their non-mannosylated variants (Table 1), yet mannosylated polymers used to generate hybrid vectors mediated statistically higher zeta potential values regardless of buffer. This may be the result of increased surface deposition (Figure 1) that is driven by yet unknown mechanisms.

### Initial Polymer Gene Delivery and Cytotoxicity

Previously, we identified that mannosylation (either by chemical conjugation or free addition) positively affected gene delivery of polyplexes (polymer complexed to plasmid DNA [pDNA]) in direct response to binding and processing through CD206-dependent mechanisms [4]. However, given the order of magnitude size differences between polyplexes (<300 nm) and hybrid vectors (~2.5  $\mu\text{m}$ ), the effect of upon hybrid-mediated gene delivery was believed to provide a secondary mechanism to promote APCs uptake specificity. In this study, hybrid vectors were evaluated for gene delivery outcomes at a 10:1 MOI and four polymer doses (Figure 3A). Unlike our initial hybrid vector study [3], mannosylated hybrid gene delivery increased linearly with polymer dose; whereas, non-mannosylated vectors retained optimal activity at lower doses (<0.5 mg/mL). All mannosylated hybrids mediated statistical higher gene delivery values than the commercial and bacterial controls at the highest polymer dose. From this library, hybrid vectors containing D4A4-Man promoted the highest gene delivery values at every polymer dose. The differences between gene delivery outcomes between each polymer were unexpected because of the chemical background similarity across the library. Specifically, monomers were chosen from an extensive chemical background screen [3] and only differ by single carbon displacements (Figure S1). Aside from gene delivery, polymer addition improved hybrid-mediated cytotoxicity in a dose-dependent manner (Figure 3B) and with exception of a few polymers (D3mA5, D5A4, and D5A4-Man), mediated negligible cytotoxicity (>95% viability) at the highest polymer dose. Decreased cytotoxicity is the result of positive polymer degradation properties [19, 20] and charge-mediated bacterial attenuation [21].

Given the nuanced structural differences between individual polymers, the library was analyzed for a molecular weight effect upon hybrid vector gene delivery (Figure S2). Polymer molecular weight was weakly correlated ( $R^2 < 0.5$ ) with gene delivery. Furthermore, due to the small size of the library assessed coupled to an incomplete understanding of the fundamental APC-associated vector processing steps, limited information can be ascertained regarding the polymeric structural features governing hybrid vector gene delivery results. Thus, selecting D4A4-Man as the base chemical background (the most effective polymer above), we synthesized a library of second-generation stratified molecular weight polymers

(Table 2 and Figure S3). By doing so, the library can be assessed for structure-function relationships by systematically characterizing gene delivery as a function of (1) polymer molecular weight, (2) relative mannose content, (3) polymer-membrane biophysical properties, (4) APC uptake specificity, and (5) serum inhibition.

### Expanded D4A4-Man Library Assessments

The expanded D4A4-Man library introduces the same chemical background to each polymer, enabling the direct assessment of structural parameters that include polymer molecular weight and mannosylation in hybrid vector formation and subsequent gene delivery outcomes. Using the same transfection strategy described above, hybrid vectors were formed using four polymer doses and a 10:1 MOI (Figure 4). Hybrid gene delivery increased linearly in reference to increasing polymer dose and decreasing molecular weight. Interestingly, polymers with numbered molecular weights below 10 kDa (P7-P14) mediated gene delivery values statistically higher than commercial and bacterial controls at all polymer doses. In addition, gene delivery gradually increased with molecular weight decreases before plateauing at 5.5 kDa. Below this polymer molecular weight, there are no statistical differences between polymers, regardless of dose, in gene delivery.

To aid the understanding of the observed gene delivery trends, biophysical characterization was conducted as described above to evaluate the effects of polymer molecular weight on bacterial surface properties (Figure S4). Bacterial membrane coverage (Figure S4A) and integrity (Figure S4B) were governed by inverse polymer molecular weight trends. Specifically, lower weight polymers mediated the highest surface coverage; whereas, higher weight polymers mediated the highest membrane destabilization. These observations may be the result of concomitant increases in membrane destabilization potential with increasing polymer molecular weight. This hypothesis is based by the understanding that higher molecular weight polymers possess the highest amine content, which, when introduced to an acidic environment (e.g., the hybrid vector complexation buffer [25 mM NaOAc, pH 5.15]), prompts charge-dependent lipid bilayer disruption similar to other bactericidal agents (e.g., polymyxin B) [7, 22].

In order for the mannosylated hybrid to be successful in translational applications, these vectors must possess the innate ability to overcome the barriers present during administration. That stated, key limitations include target specificity and the documented loss-of-activity that accompanies vectors in the presence of physiological levels of extracellular protein [2]. Failure of vectors to traverse these hurdles results in significant off-target effects, premature aggregation, degradation, and subsequent clearance [23, 24]. As such, transfection was conducted using 1.0 mg/mL hybrids at 10:1 MOI in the presence of CD206-inhibiting concentrations of free mannose and/or physiologically-relevant level of serum (Figure 4B). All hybrids exhibited significant drops in transfection due to both mannose and serum inhibitions. However, decreasing polymer molecular weight resulted in the formation of hybrids that were increasingly sensitive to mannose inhibition and decreasingly sensitive to serum inhibition (Figure S5). Furthermore, in the simultaneous presence of mannose and serum, inhibition resulted in a maximization effect of gene delivery. Specifically, moderate molecular weights (P8–P11) retained gene delivery



capabilities surpassing optimal commercial and bacterial controls (transfected in non-physiological conditions; thus these control values represent maximums). This may be the result of a balancing effect between excess charge density present on higher molecular weight polymers (which prompts increased serum deposition due to electrostatic interactions) and increased relative mannose content of lower molecular weight polymers (per unit volume). Collectively, these results suggest translational APC-targeting hybrid vectors should be designed to include moderately charged and moderate molecular weight variants such as P11.

In our previous studies of delivering pDNA via mannosylated polyplexes, we observed mannose-mediated uptake resulted in endocytic processing that was more permissive to gene delivery. Furthermore, mannose-mediated processing (through CD206 mechanisms) is associated with endocytic trafficking towards recycling mechanisms [25, 26] and through proposed additional endocytic vesicles (early to late endosome) [27]. We previously concluded that increased efficacy may have also been the result of triggering uptake and processing mechanisms that were either bypassing degradative compartments of the cell [28–31] or escaping endocytic recycling mechanisms [26]. However, given the size associated with our hybrid device, uptake is restricted to phagocytic mechanisms (Figure 5A) and cannot take advantage of general uptake (Figure 5B–D). Interestingly, other studies have highlighted the harsh nature of processing through general phagocytosis, indicating minor biomolecule release representing less than 5% of processed cargo [32]. Thus, the role of mannosylation upon hybrid-mediated processing is not completely clear. That said, mannosylation of hybrids is triggering uptake and processing mechanisms beneficial to eventual gene delivery that may not be governed by the same polymeric structure-function rules associated with general uptake mechanisms.

Nevertheless, increased gene delivery activity may be rooted in the nature of the mannose receptor (MR). Even though MR-mediated phagocytosis is poorly understood, the innate activity of this processing pathway is directed against pathogenic microbes which are coated with mannose-containing structures [33]. Furthermore, instigation of this receptor is known to increase antigen presentation activity in vaccine efforts [34–36] by intensifying recruitment of degradative components (e.g., lysozyme and proteases) [37]. However, intracellular pathogens are known to take advantage of the increased degradative activity by the over-expression of pH-dependent hemolysin proteins [37, 38]. Given the current design of the bacterial-component of the hybrid vector to heterologously express the pH-dependent hemolysin, LLO, increased degradative activity should increase resulting gene delivery responses. The combination of mannosylation with the engineered bacterial core provides an additional demonstration of the dual flexibility in the generation of hybrid vectors that possess new levels of biomimicry.

## CONCLUSION

The library of polymers developed in this study highlights the ability of moderately sized and charged mannosylated PBAEs to form hybrid bio-synthetic vectors that are capable of mediating effective transfection to APCs in physiological conditions. Taken together, the

study provides the first report of polymer structure-function relationships that can be readily applied to all future hybrid bio-synthetic gene delivery studies.

## Supplementary Material

Refer to Web version on PubMed Central for supplementary material.

## Acknowledgments

### Funding Sources

The authors recognize support from NIH award AI088485 (BAP) and a SUNY-Buffalo Schomburg fellowship (CHJ).

## REFERENCES

1. Jones CH, Hakansson AP, Pfeifer BA. Biomaterials at the interface of nano- and micro-scale vector-cellular interactions in genetic vaccine design. *Journal of Materials Chemistry B*. 2014; 2:8053–8068.
2. Jones CH, Chen CK, Ravikrishnan A, Rane S, Pfeifer BA. Overcoming nonviral gene delivery barriers: perspective and future. *Mol Pharm*. 2013; 10:4082–4098. [PubMed: 24093932]
3. Jones CH, Ravikrishnan A, Chen M, Reddinger R, Kamal Ahmadi M, Rane S, et al. Hybrid biosynthetic gene therapy vector development and dual engineering capacity. *Proc Natl Acad Sci U S A*. 2014; 111:12360–12365. [PubMed: 25114239]
4. Jones CH, Chen M, Ravikrishnan A, Reddinger R, Zhang G, Hakansson AP, et al. Mannosylated poly(beta-amino esters) for targeted antigen presenting cell immune modulation. *Biomaterials*. 2015; 37:333–344. [PubMed: 25453962]
5. Little SR, Lynn DM, Ge Q, Anderson DG, Puram SV, Chen J, et al. Poly-beta amino ester-containing microparticles enhance the activity of nonviral genetic vaccines. *Proc Natl Acad Sci U S A*. 2004; 101:9534–9539. [PubMed: 15210954]
6. Little SR, Lynn DM, Puram SV, Langer R. Formulation and characterization of poly (beta amino ester) microparticles for genetic vaccine delivery. *J Control Release*. 2005; 107:449–462. [PubMed: 16112767]
7. Jones CH, Rane S, Patt E, Ravikrishnan A, Chen CK, Cheng C, et al. Polymyxin B treatment improves bacterofection efficacy and reduces cytotoxicity. *Mol Pharm*. 2013; 10:4301–4308. [PubMed: 24093973]
8. Parsa S, Wang Y, Rines K, Pfeifer BA. A high-throughput comparison of recombinant gene expression parameters for *E. coli*-mediated gene transfer to P388D1 macrophage cells. *J Biotechnol*. 2008; 137:59–64. [PubMed: 18694790]
9. Parsa S, Wang Y, Fuller J, Langer R, Pfeifer BA. A comparison between polymeric microsphere and bacterial vectors for macrophage P388D1 gene delivery. *Pharm Res*. 2008; 25:1202–1208. [PubMed: 18343983]
10. Mena MA, Treynor TP, Mayo SL, Daugherty PS. Blue fluorescent proteins with enhanced brightness and photostability from a structurally targeted library. *Nature Biotechnology*. 2006; 24:1569–1571.
11. Rosenberg M. Microbial adhesion to hydrocarbons: twenty-five years of doing MATH. *FEMS microbiology letters*. 2006; 262:129–134. [PubMed: 16923066]
12. Geertsemadoornbusch GI, Vandermei HC, Busscher HJ. Microbial cell-surface hydrophobicity - the involvement of electrostatic interactions in microbial adhesion to hydrocarbons (Math). *Journal of Microbiological Methods*. 1993; 18:61–68.
13. Sunshine JC, Sunshine SB, Bhutto I, Handa JT, Green JJ. Poly(beta-amino ester)-nanoparticle mediated transfection of retinal pigment epithelial cells *in vitro* and *in vivo*. *Plos One*. 2012; 7:e37543. [PubMed: 22629417]

14. Sunshine JC, Peng DY, Green JJ. Uptake and transfection with polymeric nanoparticles are dependent on polymer end-group structure, but largely independent of nanoparticle physical and chemical properties. *Mol Pharm*. 2012; 9:3375–3383. [PubMed: 22970908]
15. Anderson DG, Akinc A, Hossain N, Langer R. Structure/property studies of polymeric gene delivery using a library of poly(beta-amino esters). *Mol Ther*. 2005; 11:426–434. [PubMed: 15727939]
16. Anderson DG, Lynn DM, Langer R. Semi-automated synthesis and screening of a large library of degradable cationic polymers for gene delivery. *Angewandte Chemie*. 2003; 42:3153–3158. [PubMed: 12866105]
17. Studier FW, Moffatt BA. Use of bacteriophage T7 RNA polymerase to direct selective high-level expression of cloned genes. *Journal of Molecular Biology*. 1986; 189:113–130. [PubMed: 3537305]
18. Chung TC, Jones CH, Gollakota A, Ahmadi MK, Rane S, Zhang G, et al. Improved *Escherichia coli* bactofection and cytotoxicity by heterologous expression of bacteriophage PhiX174 lysis gene E. *Mol Pharm*. 2015
19. Jones CH, Chen M, Ravikrishnan A, Reddinger R, Zhang G, Hakansson AP, et al. Mannosylated poly(beta-amino esters) for targeted antigen presenting cell immune modulation. *Biomaterials*. 2015; 37:333–344. [PubMed: 25453962]
20. Jones CH, Chen M, Gollakota A, Ravikrishnan A, Zhang G, Lin S, et al. Structure-function assessment of mannosylated poly(beta-amino esters) upon targeted antigen presenting cell gene delivery. *Biomacromolecules*. 2015
21. Jones CH, Chen CK, Chen M, Ravikrishnan A, Zhang H, Gollakota A, et al. PEGylated Cationic Poly lactides for Hybrid Biosynthetic Gene Delivery. *Mol Pharm*. 2015; 12:846–856. [PubMed: 25625426]
22. Zhu C, Yang Q, Lv F, Liu L, Wang S. Conjugated polymer-coated bacteria for multimodal intracellular and extracellular anticancer activity. *Adv Mater*. 2013; 25:1203–1208. [PubMed: 23280674]
23. Canine BF, Hatefi A. Development of recombinant cationic polymers for gene therapy research. *Adv Drug Deliv Rev*. 2010; 62:1524–1529. [PubMed: 20399239]
24. Pack DW, Hoffman AS, Pun S, Stayton PS. Design and development of polymers for gene delivery. *Nat Rev Drug Discov*. 2005; 4:581–593. [PubMed: 16052241]
25. Stahl P, Schlesinger PH, Sigardson E, Rodman JS, Lee YC. Receptor-mediated pinocytosis of mannose glycoconjugates by macrophages: characterization and evidence for receptor recycling. *Cell*. 1980; 19:207–215. [PubMed: 6766809]
26. Sahay G, Querbes W, Alabi C, Eltoukhy A, Sarkar S, Zurenko C, et al. Efficiency of siRNA delivery by lipid nanoparticles is limited by endocytic recycling. *Nature Biotechnology*. 2013
27. Simmons BM, Stahl PD, Russell JH. Mannose receptor-mediated uptake of ricin toxin and ricin A chain by macrophages. Multiple intracellular pathways for a chain translocation. *J Biol Chem*. 1986; 261:7912–7920. [PubMed: 3711116]
28. Shin JS, Abraham SN. Cell biology. Caveolae--not just craters in the cellular landscape. *Science*. 2001; 293:1447–1448. [PubMed: 11520975]
29. Pelkmans L, Helenius A. Endocytosis via caveolae. *Traffic*. 2002; 3:311–320. [PubMed: 11967125]
30. Parton RG, Simons K. The multiple faces of caveolae. *Nature Reviews Molecular Cell Biology*. 2007; 8:185–194. [PubMed: 17318224]
31. Rehman Z, Zuhorn IS, Hoekstra D. How cationic lipids transfer nucleic acids into cells and across cellular membranes: recent advances. *J Control Release*. 2013; 166:46–56. [PubMed: 23266451]
32. Gage E, Hernandez MO, O'Hara JM, McCarthy EA, Mantis NJ. Role of the mannose receptor (CD206) in innate immunity to ricin toxin. *Toxins*. 2011; 3:1131–1145. [PubMed: 22069759]
33. Medzhitov R. Recognition of microorganisms and activation of the immune response. *Nature*. 2007; 449:819–826. [PubMed: 17943118]
34. Carrillo-Conde B, Song EH, Chavez-Santoscoy A, Phanse Y, Ramer-Tait AE, Pohl NL, et al. Mannose-functionalized "pathogen-like" polyanhydride nanoparticles target C-type lectin receptors on dendritic cells. *Mol Pharm*. 2011; 8:1877–1886. [PubMed: 21882825]

35. Chavez-Santoscoy AV, Roychoudhury R, Pohl NL, Wannemuehler MJ, Narasimhan B, Ramer-Tait AE. Tailoring the immune response by targeting C-type lectin receptors on alveolar macrophages using "pathogen-like" amphiphilic polyanhydride nanoparticles. *Biomaterials*. 2012; 33:4762–4772. [PubMed: 22465338]
36. Prigozy TI, Sieling PA, Clemens D, Stewart PL, Behar SM, Porcelli SA, et al. The mannose receptor delivers lipoglycan antigens to endosomes for presentation to T cells by CD1b molecules. *Immunity*. 1997; 6:187–197. [PubMed: 9047240]
37. Stahl PD, Ezekowitz RA. The mannose receptor is a pattern recognition receptor involved in host defense. *Current Opinion in Immunology*. 1998; 10:50–55. [PubMed: 9523111]
38. Parsa S, Pfeifer B. Engineering bacterial vectors for delivery of genes and proteins to antigen-presenting cells. *Mol Pharm*. 2007; 4:4–17. [PubMed: 17233543]

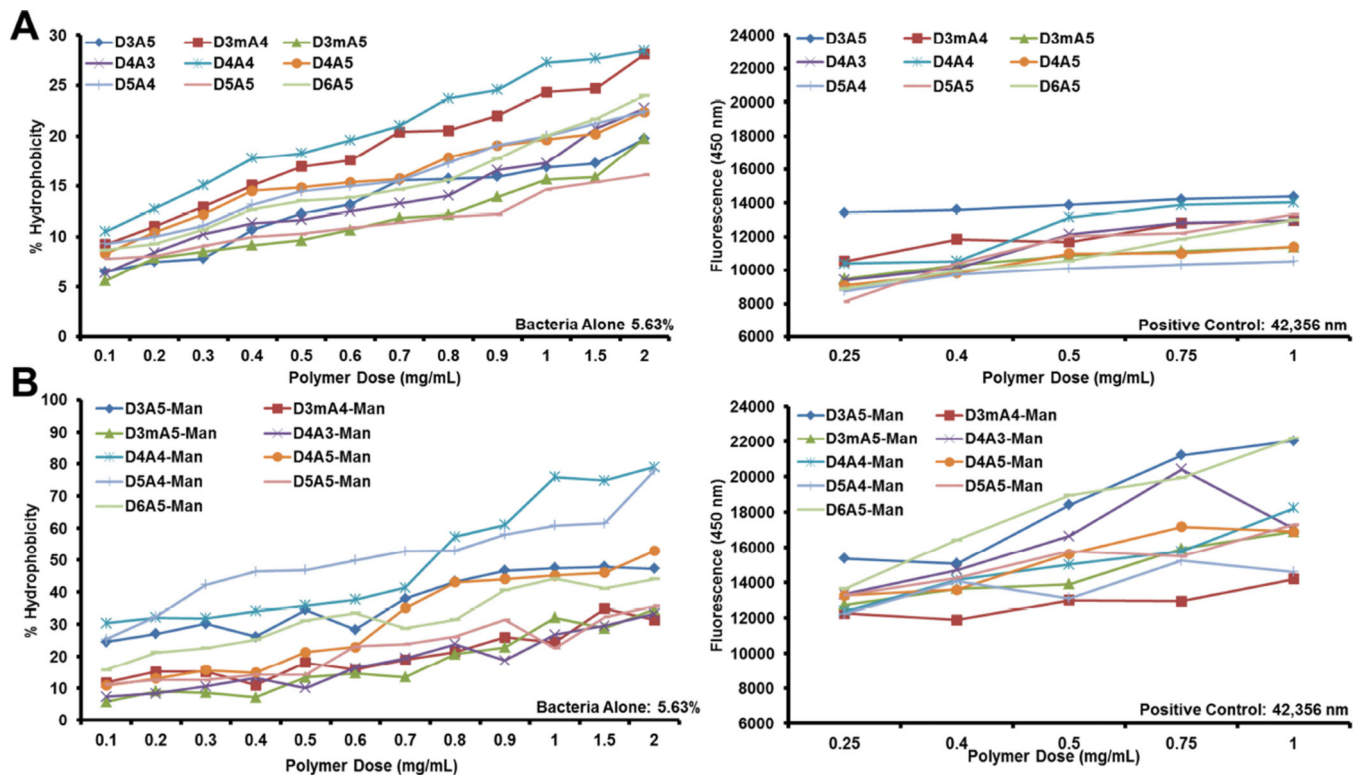


**Figure 1.** Hybrid vector characterization. Effects of surface addition of non-mannosylated (A) and mannosylated (B) PBAEs upon bacterial hydrophobicity (left panels) and membrane shearing (right panels). In membrane shearing studies, the positive control represents treatment of unmodified bacterial vectors with polymyxin B.

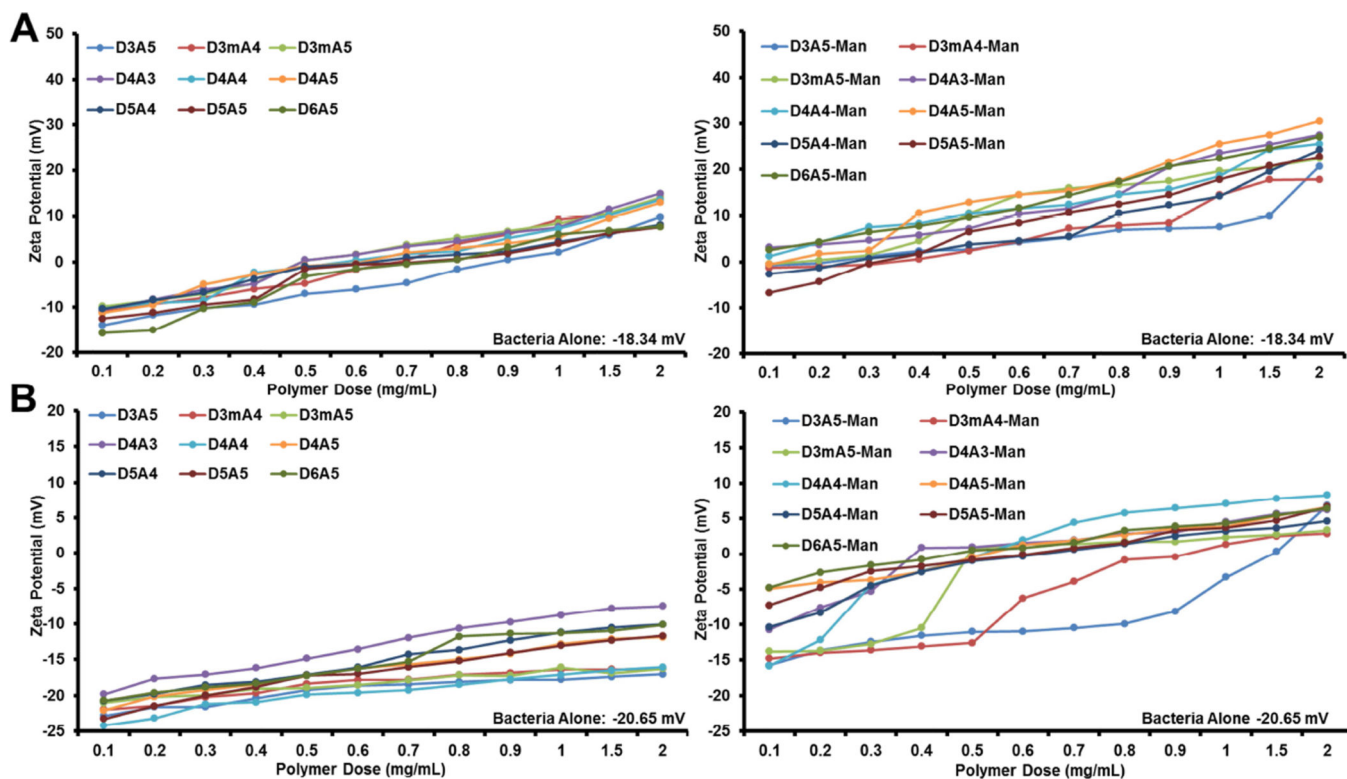


**Figure 2.** Additional hybrid vector characterization. Zeta potential measurements of various surface additions of non-mannosylated and mannosylated PBAEs in 25 mM NaOAc (pH 5.15; A) and PBS (pH 7.4; B). All mannosylated readings were statistically higher than non-mannosylated variants (95% confidence).

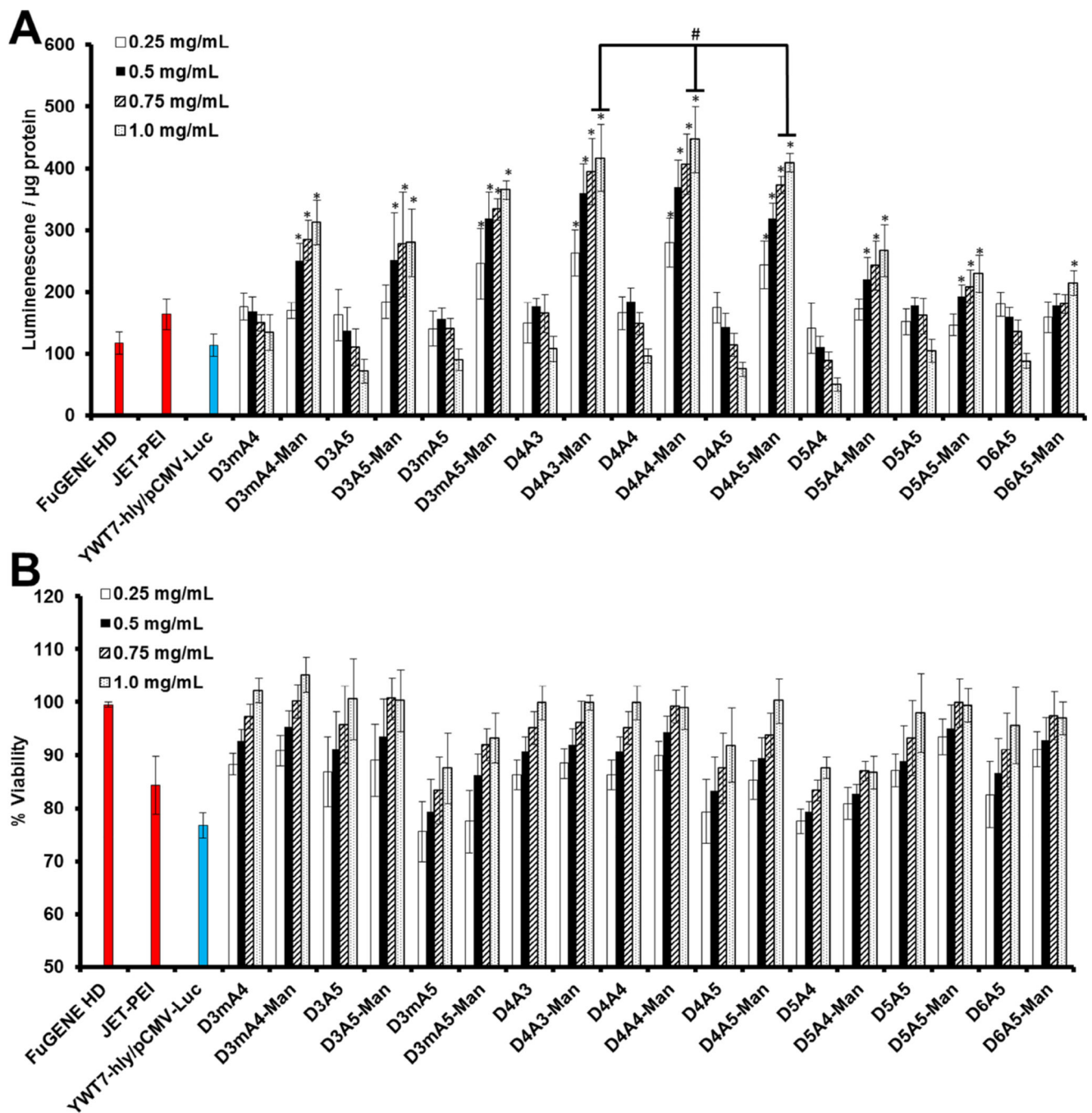


**Figure 3.** Gene delivery and toxicity assessment. Hybrid vectors were prepared with various doses of polymers and evaluated for gene delivery (A) and cytotoxicity (B). All transfections utilized a 10:1 MOI. \*Indicates statistical improvements (95% confidence) compared to commercial and bacterial controls. #Indicates statistical improvements (95%) compared to all other hybrid vectors (excluding D4A3-Man, D4A4-Man, and D4A5-Man) at that particular polymer dose (1.0 mg/mL).

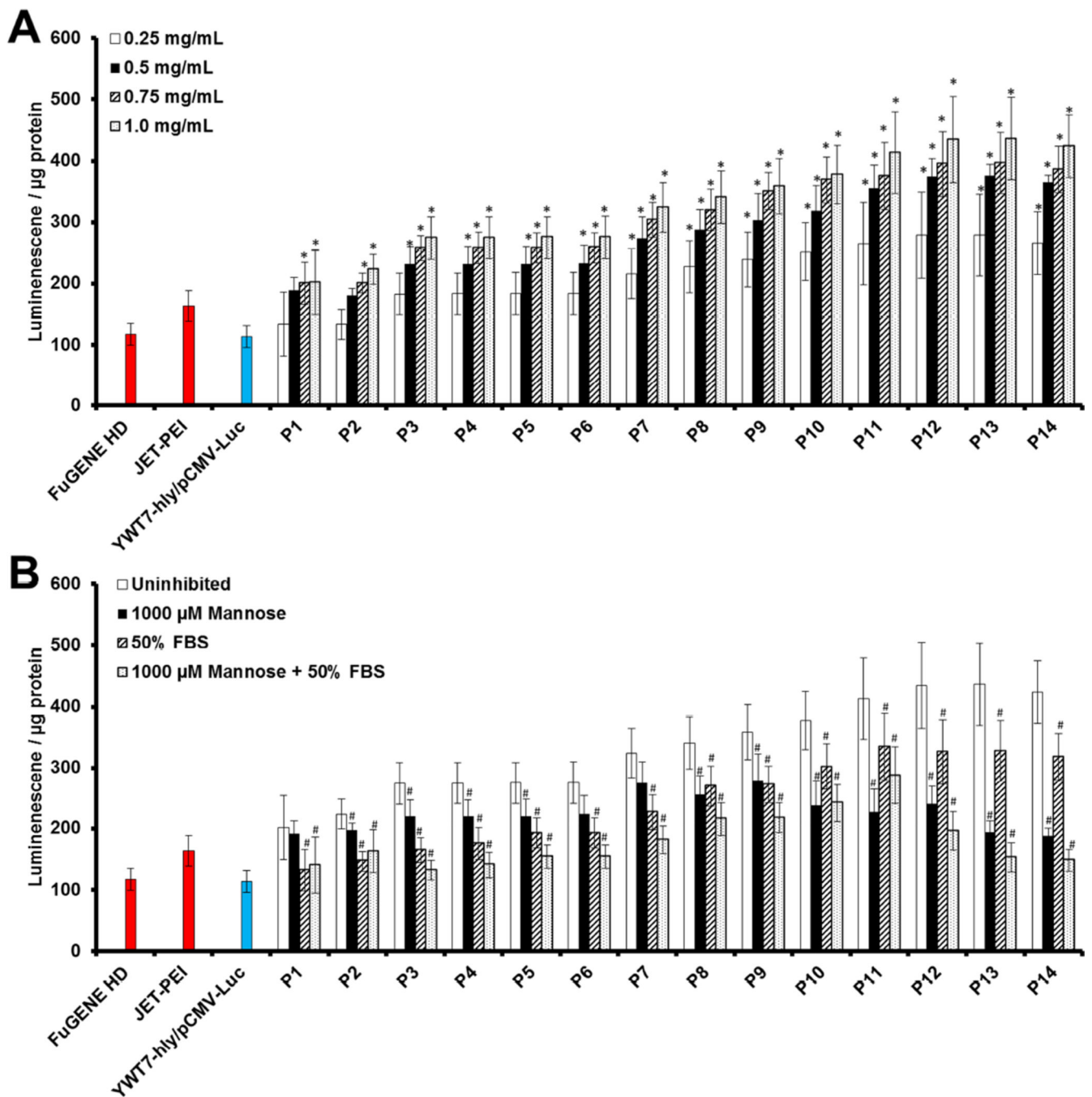


**Figure 4.** Expanded gene delivery using different molecular weight D4A4-Mans at a 10:1 MOI. Hybrid vectors composed of different polymer doses were evaluated for gene delivery (A). Gene delivery was then analyzed in the presence of free mannose and/or physiologically-relevant levels of FBS (B). \*Indicates statistical improvements (95% confidence) compared to commercial and bacterial controls. #Indicates statistical decrease (95% confidence) between samples compared to respective uninhibited transfection. Mannose and serum



inhibited gene delivery values of P8-P11 are statistically higher (95% confidence) compare to commercial and bacterial controls.

Author Manuscript

Author Manuscript

Author Manuscript

Author Manuscript

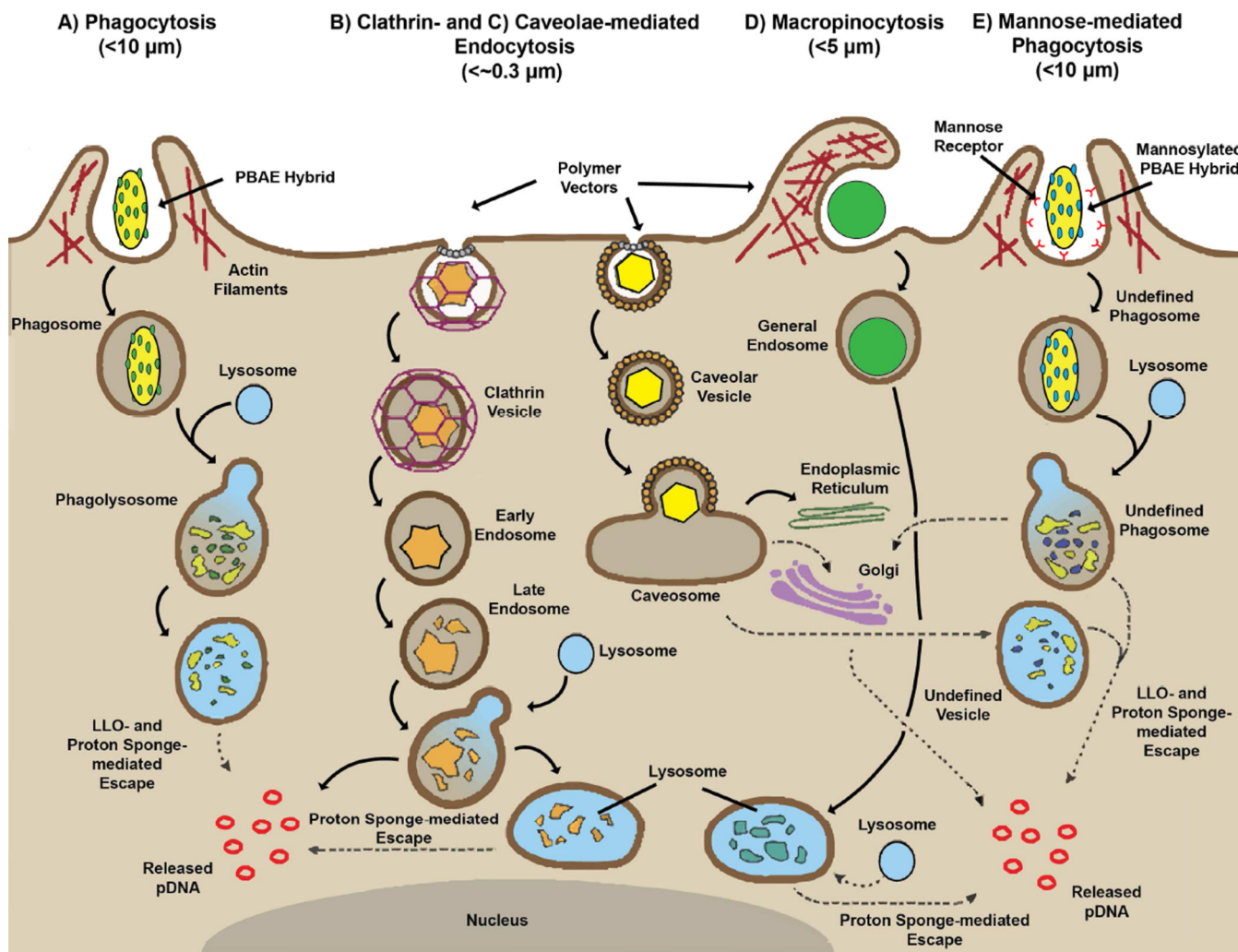


**Figure 5.**

Proposed uptake mechanism of mannosylated hybrid bio-synthetic gene delivery vectors. General steps associated with uptake and processing of hybrid (A and E) and polymer-based vectors (B-D). Common to each route is the size- and receptor-mediated encapsulation of delivery vectors, followed by general acidification through the fusion of lysosomes (except in the caveolar-mediated pathway [C]). Upon acidification, each vector possesses innate escape mechanism to aid the unpackaging and release of pDNA into the cytosol for eventual nuclear translocation and expression. Polymeric components mediate release through a charge-related proton mechanism termed the “Proton Sponge” effect [24]. However, due to the duality of the hybrid vectors, there is an additional biologically-based escape mechanism that mediates independent release. This biological escape mechanism is a non-native pore-forming peptide, listeriolysin O, which has been engineered and specifically introduced into the hybrid bacterial core.

**Table 1**

Polymer Synthesis and Characterization Summary of Base Polymers

Polymer	PD <sub>1</sub> <sup>GPC</sup>	M <sub>n</sub> <sup>GPC</sup> (Da)	M <sub>w</sub> <sup>GPC</sup> (Da)	Zeta Potential (mV) PBS (pH 7.4)	Zeta Potential (mV) NaOAc (pH 5.15)
D3mA4	1.342	7,839	10,520	-19.4	28.8
D3mA4-Man	1.696	6,996	11,863	-6.4	20.1
D3A5	1.418	8,214	11,643	-18.6	37.5
D3A5-Man	1.640	5,083	8,337	-4.1	31.7
D3mA5	1.206	8,848	10,667	-19.9	33.1
D3mA5-Man	1.574	8,128	12,794	-12.6	28.7
D4A3	1.405	9,617	13,511	-12.5	34.5
D4A3-Man	1.680	4,403	7,397	-9.9	28.6
D4A4	1.629	8,571	13,961	-19.5	25.9
D4A4-Man	1.377	4,967	6,839	-12.4	20.6
D4A5	1.453	8,520	12,380	-16.7	28.5
D4A5-Man	1.542	4,762	7,345	-11.2	34.2
D5A4	1.377	8,927	12,294	-12.7	21.2
D5A4-Man	1.622	8,701	14,109	-8.4	26.3
D5A5	1.319	9,577	12,632	-26.0	31.1
D5A5-Man	1.501	7,040	10,567	-15.5	25.5
D6A5	1.472	8,286	12,198	-21.8	34.2
D6A5-Man	1.664	7,517	12,508	-18.4	33.4

**Table 2**  
 Synthesis and characterization summary of molecular weight variants of D4A4-Man

Polymer Designation	D4:A4 Feed Ratio	PD <sub>i</sub> GPC	M <sub>n</sub> GPC (Da)	M <sub>w</sub> GPC (Da)	Zeta Potential (mV) PBS (pH 7.4)	Zeta Potential (mV) NaOAc (pH 5.15)
P1	1.025	2.477	13,623	33,745	-8.6	32.6
P2	1.0375	1.641	13,425	22,031	-5.3	34.0
P3	1.05	1.536	11,961	18,372	-6.2	33.6
P4	1.0625	1.370	11,848	16,232	-8.3	32.4
P5	1.075	1.629	10,474	17,063	-7.7	32.7
P6	1.1	1.642	10,130	16,633	-8.8	34.6
P7	1.125	1.833	7,902	14,484	-8.0	31.9
P8	1.15	1.468	7,312	10,734	-11.1	27.5
P9	1.175	1.699	6,589	11,195	-12.1	28.6
P10	1.2	1.549	5,966	9,241	-11.2	24.9
P11	1.225	1.590	5,510	8,761	-11.4	26.4
P12	1.25	1.600	5,112	8,180	-12.7	24.0
P13	1.275	1.638	4,673	7,654	-12.9	20.9
P14	1.3	1.615	4,479	7,234	-11.2	21.4